CHAOS
Theory and Applications
in Applied Sciences and Engineering

e-ISSN: 2687-4539
RESEARCH ARTICLE
Vol.4 / No.4 / 2022 / pp.226-233
Special Issue (EDIESCA 2022)
https://doi.org/10.51537/chaos.1197559

Effects of Optical Laser Injection in Multistable Erbium Fiber Lasers

J.O. Esqueda-de-la-Torre *,1, **R. Jaimes-Reátegui** *,2, **J.H. García-López** *,3, **A. N. Pisarchik** β,4 **and G. Huerta-Cuellar** *,5

*Dynamical Systems Laboratory, Centro Universitario de los Lagos, Universidad de Guadalajara, Enrique Díaz de León 1144, Paseos de la Montaña, 47460, Lagos de Moreno, Jalisco, Mexico , βCenter for Biomedical Technology, Technical University of Madrid, Campus Montegancedo, 28223 Pozuelo de Alarcón, Madrid, Spain.

ABSTRACT During the past years, the study of optical injection has been intensely carried in theoretical and experimental realizations, showing interesting emergent behaviors, and synchronized states between other results. This work proposes an experimental scheme of an array of three driven erbium-doped fiber lasers (EDFLs), which dynamics exhibit the coexistence of multiple attractors. The laser array is controlled by a driver EDFL by injecting its optical intensity into the three coupled driven EDFLs array. The experimental realization was with the aim to induce an attractor tracking in the driving lasers, then to get coexisting states with increasing output power, and to study other emergent behavior given by the differences between doped fibers. To find the multistability regions, some bifurcation diagrams of the laser peak intensities are constructed. The obtained results are identified by comparing them with the modulation frequency. In some cases, the obtained results show that the intensity of the optical output signal of the driven systems is increased with respect to the initial individual response. In the case of synchronized states, it's possible to get an increased signal from the whole system. The obtained results could have important applications in repeaters of communications systems.

KEYWORDS
Erbium doped fiber laser
Multistability
Coupling
Non-linearity
Power increase

INTRODUCTION

Since some years ago, a rapid increase has been achieved in commercialization and research on erbium-doped fiber laser (EDFLs). This devices have been studied extensively for their flexible applications in several important optical systems as optical communications, laser surgery, nonlinear optics, optical sensing, and optical materials (Digonnet 2001; Luo and Chu 1998; Duarte 2009; Pisarchik *et al.* 2013; R. Mary and Kar 2014; Zhao *et al.* 2017). The EDFL active gain medium offers a long interaction length of pump light because the active ions that lead to a single transversal operation mode and a high gain produced by the correct choice of fiber parameters (Kir'yanov *et al.* 2013). Moreover, the signal amplification in optical fibers offers great advantages for technological applications due to its particular characteristics like electromagnetic field robustness, efficiency, reliability, compactness with an additional alignment-free structure, and spatial beam profile (Liu *et al.* 2020; Jafry *et al.* 2020). In that sense, the optical power increase is in constant evolution for the implementation of better fiber optical amplifiers capable of transmitting a signal in a fiber optical network along hundreds of kilometers with a minimum attenuation (Bouzid 2011).

It is well known that EDFL amplifiers wavelength, especially 1550 nm, shows very small losses in optical fibers (Castillo-Guzmán *et al.* 2008), as well as, a very rich dynamical behavior that the EDFL can exhibit (chaos, multistability, period-doubling,,etc.) (Reategui *et al.* 2004; Huerta-Cuellar *et al.* 2008) that can be have applications in different applications, such as, e.g., industrial micromachining (Kraus *et al.* 2010), medicine (Morin *et al.* 2009), spectral interferometry (Keren and Horowitz 2001), optical sensing (Wu *et al.* 2014), optical coherence tomography (Lim *et al.* 2005), optical metrology (Droste *et al.* 2016), and LiDAR systems (Philippov *et al.* 2004). In such systems, a particular state is determined by initial conditions (Pisarchik *et al.* 2005, 2011).

Manuscript received: 3 November 2022,
Revised: 28 November 2022,
Accepted: 29 November 2022.

[1]jose.edelatorre@alumnos.udg.mx
[2]rider.jaimes@academicos.udg.mx
[3]jhugo.garcia@academicos.udg.mx
[4]alexander.pisarchik@ctb.upm.es
[5]guillermo.huerta@academicos.udg.mx (**Corresponding author**).

Among many results showing the nonlinear behavior in EDFLs, few researchers are interested in the study of multistability in these lasers (Reategui *et al.* 2004; Huerta-Cuellar *et al.* 2008; Pisarchik *et al.* 2005; Huerta-Cuellar *et al.* 2009). EDFL's can exhibit up to four coexisting states under periodic modulation of the pump laser, in this sense, a high period attractor contains a high pulse energy (Pisarchik *et al.* 2011). Some other results in multistable systems show the possibility to obtain a monostable behavior by eliminating undesirable attractors, and in that sense some methods and results on attractor annihilation have been shown Sevilla-Escoboza *et al.* (2017); Pisarchik and Jaimes-Reategui (2009); Magallón *et al.* (2022). Recently Barba-Franco *et al.* (2023), shown the implementation of an electronical version of an EDFL based on differential equations.

The phenomenon of optical injection in lasers have been extensively studied since more than twenty years ago, and some recent results have been reported in VCSEL's Doumbia *et al.* (2022), showing the nonlinear dynamics and the polarization properties of a VCSEL by using a frequency comb. Between interesting results in the case of optical injection in semiconductor lasers, extreme events (EEs) have been recently investigated, and the probability of appearance of EEs can be controlled by the injection parameters applied to the locking regions of the diver-driving laser configuration (Huang *et al.* 2022). In the case of numerical injected semiconductor lasers modelated by the Lang-Kobayashi equations, different noise-induced transitions have been reported Tseng *et al.* (2022). Erbium doped fiber lasers has show different behaviors when optical injection is performed in this devices. In Xu *et al.* (2022), experimentally observed the evolutionary dynamics of convention solitons(CSs) in a simplified Erbium-doped fiber laser. An interesting phenomenon known as Q-switching was recently reported by Cai *et al.* (2022), they shown that the pulse evolution and dynamics of a pulsed erbium-doped fiber laser with plasmonic titanium nitride nanoparticles under different pump powers can result in two states: mode-locking and Q-switched mode-locking (QS-ML). Aditionally, the presence of noise-like behavior in doped fiber laser is one of the most interesting phenomena when the lasers are operating in a mode-looking regime, some results in this topic was presented by Soboń (2022).

Reported results about EDFL's injection shows the apparition of energetic pulses and some applications as the mentioned Q-switching phenomenon for certain laser type, but the dynamical response of a fiber laser depends on the doped level, and the distribution of the doping atoms in the fiber material as reported by Kir'yanov *et al.* (2013). In that sense, each of the implemented driven lasers were constructed with the same erbium doped fiber, but with different segments of fiber. With the aim of study the different possible behaviors when each of the EDFL's are injected by the driver EDFL, and looking for a high power emission in multistable EDFLs array, an experimental study of a four lasers system is implemented. Despite the existence of different results reported by injection into erbium-doped fiber lasers, this paper compares differences that may exist when using lasers implemented with different sections of the same doped fiber. The experimental setup is constructed by using a multistable driver EFDL Huerta-Cuellar *et al.* (2008), that injects an optical signal of a controlled state to three coupled multistable EFDLs.

This next sections of this paper is structured as follows. In Section 2, numerical model, materials and methods, the tools and basics of this work are shown, section 3, is about the experimental obtained results, and its discussion. Finally, the main conclusions of this work are given in section 4.

METHODS AND MATERIALS

Mathematical model

As first part of this research work, the model aproximation of the experimental setup is studied. The mathematical model of one normalized EDFL equations is shown in eq. 1:

$$\begin{aligned} \frac{dx}{dt} &= axy - bx + c(y + 0.3075), \\ \frac{dy}{dt} &= -\delta xy - (y + 0.3075) + ... \\ ... \; & P_{pump}(1 - exp(-18(1 - (y + 0.3075)/0.6150))), \end{aligned} \tag{1}$$

where the laser intensity is represented by x, the population inversion by y, the constants have the next values: $a = 6.6206 \times 10^7$, $b = 7.4151 \times 10^6$, $c = 0.0163$, and $\delta = 4.0763 \times 10^3$. The numerical model presented in 1, can reproduce periodic behavior depending on the combination of the initial conditions with the frequency of modulation for the bistable and multistable regions (as shown in 1(c))), and chaotic behavior as shown in Figure 1(a) for a modulation frequency (F_m), $0 < F_m < 12kHz$. Being a nonautonomous dynamic system, a pump function is required which is represented by eq. 2 where P_{pump} is the pump power, m is the modulation amplitude, and F_m is the modulation frequency.

$$P_{pump} = 506(1 + m * sin(2\phi F_m t)) \tag{2}$$

To obtain the numerical results, the Runge-Kutta method of 4^{th} order is implemented as in Reategui *et al.* (2004). As first annalysis of this laser model, a bifurcation diagram (BD) of local maxima of time series of the laser intensity x is constructed, as shown in Figure 1(a), as in Pisarchik *et al.* (2012); Esqueda-de-la Torre *et al.* (2022). This BD is obtained by sweeping the modulation frequency in a range $1kHz < F_m < 100kHz$, and by changing 30 times the initial conditions of the system. In this figure, the multistability region is obtained for a modulation frequency of $73kHz < F_m < 80kHz$ and $m = 1$ for which is $F_m = 84kHz$ is selected to generate the information of Figure 1(b), and (c), four labeled branches are distinguished for period one (P1), period three (P3), period four (P4), and period five (5) behavior, which represents coexistent states or multistable attractor. For the mentioned frequency $F_m = 80kHz$, in Figure 1(b), four time series of these coexistent attractors are shown with the pump power modulation signal P_{pump}, the ratio of the periodic attractors P1, P3, P4 and P5, are subharmonics of the modulation frequency F_m, respectively $\frac{P1}{F_m} = 1$, $\frac{P3}{F_m} = \frac{1}{3}$, $\frac{P4}{F_m} = \frac{1}{4}$, and $\frac{P5}{F_m} = \frac{1}{5}$, where P5 represents the higher intensity atractor. The Figure 1(c) shows the basin of attraction of the equation 1, with $F_m = 80kHz$, here, the colors yellow, red, blue, and green represent the initial conditions (x_0, y_0) where the EDFL shows periodic behavior represented by P1, P3, P4 and P5 respectively. Intial conditions (I.C.) used to obtain the periodical series shown in Figure 1(c), are the mentioned in table 1.

Table 1 Initial conditions used to get the periodic behavior shown in Figure 1(b).

	P1	P3	P4	P5
I.C. (x)	7.0614	24.2265	5.987	91.1913
I.C. (y)	0.0095	0.0542	0.0187	0.096

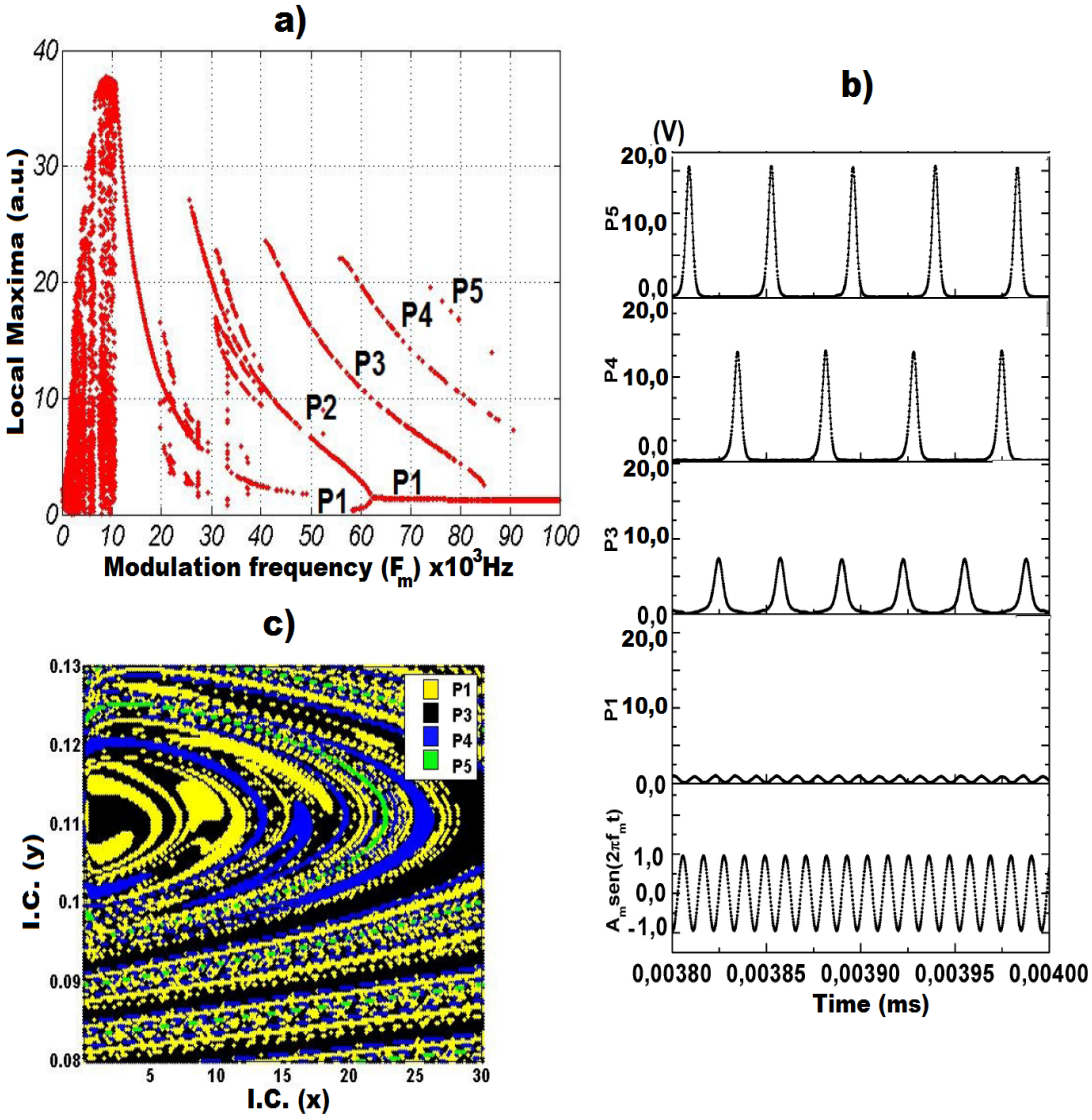

Figure 1 a) bifurcation diagram of the driver EDFL behavior , b) time series of multistable states, and pump frequency for a F_m= 80 kHz, and c) basin of attraction of the driver EDFL existing states for F_m= 80 kHz.

Experimental setup

The experimental setup of this work is shown in Figure 2, and is defined as in Esqueda-de-la Torre *et al.* (2022). The equipment and materials used are three temperature controllers ITC510, four function generators AFG3021B conected to the driver EDFL, four laser diodes BL976-PAG500, four EDFLs, eigth 1550nm Bragg gratings, four 980/1550nm wavelength divisor multiplexors WD9860BA, four photodetectors PBD481-AC, one data acquisition card NI BNC-2110, an Optical Attenuator and, a personal computer.

The driver laser (ML) which injects its optical power to the array of three erbium doped fiber lasers (SL's) is shown in Figure 2 (i). The bifurcation diagram of this laser is shown in Figure 3 (d). It has been chosen as driver due it has the richest dynamics over all the characterized lasers, showing a multistable behavior containing 5 behaviors. The injected information from the ML to the SLs could given by the for possible periodic states in the region of multistability, but in the presented results just the P5 and P4 behavior were used. It has its own function generator, current and temperature driver, a cavity and its output, as shown in Figure 2 (i).

Figure 2 (ii) shows an optical attenuator used to control the intensity of the driver laser signal, definning as coupling strength. The laser intensity variate by the optical attenuator from 8.5 V to 0 V, that corresponds to an attenuation from 0% to 100% respectively. Figures 2 (iii), (iv), and (v) represent the experimental implementation of each erbium-doped fiber driving lasers (SL's) whose bifurcation diagrams are shown in Figure 3 (a), (b), and (c) respectively. Each current Driver is being modulated by adding both the function generator and the coupling of the driver laser signal.

Figure 2 (vi) shows the data acquisition card (DAQ), previously configured in the PC to acquire the time series coming from the output optical detectors of the three erbium doped fiber driving lasers and the driver laser. In Figure 2 (vii) a personal computer appears, where all time series of the whole system are saved and analyzed to study their dynamics.

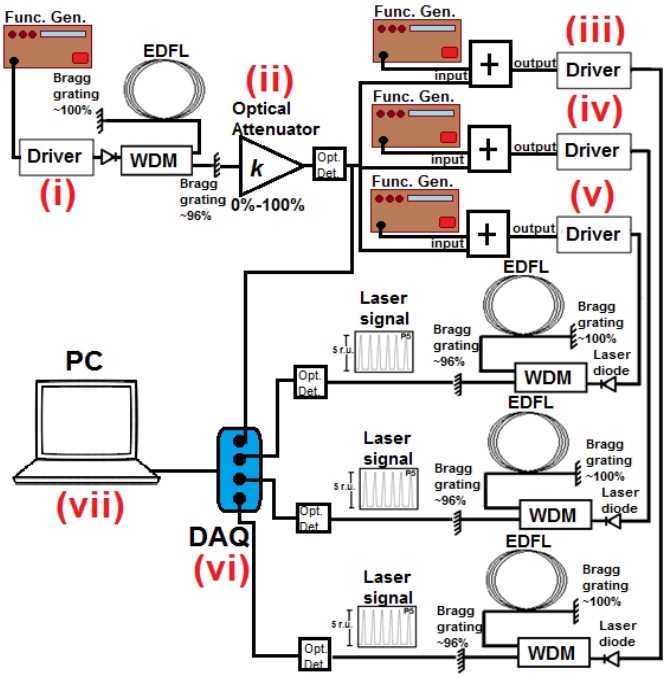

Figure 2 Experimental setup.

In the present work, the three SLs are constructed with commercial erbium doped fibers defined as type M5 Kir'yanov *et al.* (2013), and the ML is constructed by a highly doped erbium fiber laser wich presents a rich dynamical behavior as the obtained in Fig. 2 Pisarchik *et al.* (2012). As part of the characterization of the different EDFLs in this work, and in spite of the four EDFLs used in experiments are close in fiber type, and fiber measures, a bifurcation diagram of local maxima of time series for each EDFL is constructed, as shown in Huerta-Cuellar *et al.* (2008). In order to understand the behavior, modulation frequency ranges, and the multistability regime for each EDFL, the experimental bifurcation diagrams are shown in Figure 3.

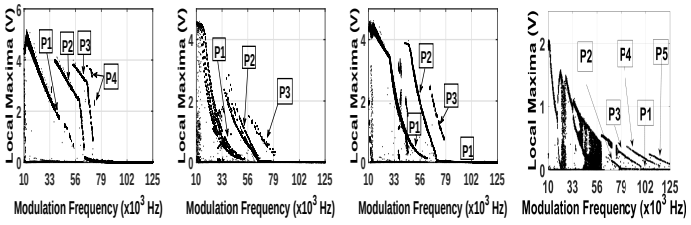

Figure 3 Bifurcation diagrams corresponding to to (a) SL1, (b) SL2, (c) SL3, and (d) ML.

RESULTS

In this section, experimental obtained results are shown. To guarantee that the behavior of the SLs is different to the behavior of the ML, each initial behavior (I.C.) is manually fixed by turning on and off the function generators shown in Figure 2(iii-v). As the results are obtained from the experimental setup, it isn't possible to know exactly the I. C. value, as in the case of numerical implementation. All of the different periodic behaviors in the EDFLs have dissimilar probability as shown in Pisarchik *et al.* (2012). From the later, is easy to obtain a P1 behavior, and it is difficult to obtain a P5 behavior, as has been experimentally shown by Huerta-Cuellar et. al. in Huerta-Cuellar *et al.* (2008).

One interesting result about optical injection was theoretically and experimentally shown by Doumbia *et al.* (2020), they uses an optical frequency comb to inject to a single frequency semiconductor, from that they obtained several dynamic behavior from periodical to chaos and other behaviors. Some dynamical effects of optical injection in multistable lasers has been recently considered by Pisarchik and Hramov (2022), from which the dynamical answer of optical injection is studied from gas lasers, semiconductor lasers, and VCELs.

Few works are devoted to studying the effects of optical injection in EDFLs. In this work, the dynamical response from three different injected EDFLs, whose were constructed from the same erbium-doped fiber are shown. The obtained results are ordered considering some of the different combinations, first by fixing the driven laser in P5 dynamics, and then it is fixed in P4, for each of the driving EDFLs (SLs), by showing what happens for each scenario for different coupling strengths. Experimental results whit coupling between ML with SLs are shown in the next sub-sections.

Fixing driver laser in period five (P5) In this subsection an evaluation of the coupling strenght between the ML and the SLs is revised. The Figure 4 shows the bifurcation diagrams of local maxima of time series for the three driving lasers (SL). Each of the SLs has been modulated by the driver laser (ML) with a previously fixed signal in P5 behavior, this can be obtained by changing the initial condition by turning on and off the function generator.

Having fixed the ML in a P5 behavior it has been applied a coupling strength k variation between the ML and each of the SLs (for SL1, SL2, and SL3). From obtained results, in Table 1 its possible to observe that the coupling value k, and the modulation amplitude are not the same, it is because the differences between the SLs behaviors that can be appreciated from Fig. 3. As result of the coupling strength between the ML and the SLs, also it is possible to see that the final behavior is not a tracking attractor from SLs to ML.

For the case that the SLs are initially in P1, Fig 4(a–c), the final obtained behavior corresponds to P5, here it worths to mention that P5 is not a possible behavior in those lasers, but the SLs reach a tracking attractor. For the coupling with SLs with a behavior different from P1, i.e. P2, and P3, the resulting behavior is not a tracking attractor between ML and SLs, and aditionally, in some cases, it is chaotic.

A comparision between the SLs is realized to know the obtained behavior after the ML perturbation. In order to see if the arrangement of three SLs reach the tracking attractor of the ML, the average values of their intensities differences has been done. When the value is close to zero, it implies the tracking attractor between the ML and the SLs, see Fig. 5.

In order to compare the obtained results from the optical injection of the ML to the SLs, the sums of the resulting behaviors of the SLs are achieved. In Fig. 6(a-d), it is possible to see from the obtained results, that in the case of SLs with initial behavior of P1, the similitude does not have a big change, while with the other initial states the results are too different between the SLs and the ML.

Fixing driver laser in period five (P4) In this subsection an evaluation of the coupling strenght between the ML and the SLs is

Table 2 Behavior of the SL for threshold k for ML P5 oscillation.

Figure	threshold k	Amplitude (V)	Modulation frequency (kHz)	LS number	Initial behavior	Final behavior
4 (a)	69	0.80	110	LS1	P1	P5
4 (b)	92	1.40	110	LS2	P1	P5
4 (c)	88	1.00	110	LS3	P1	P5
4 (d)	93	0.80	66	LS1	P2	CH
4 (e)	88	1.40	65	LS2	P2	P1
4 (f)	94	1.00	66	LS3	P2	CH
4 (g)	NA	0.80	66	LS1	P3	P3
4 (h)	NA	0.80	66	LS2	P3	P3
4 (i)	84	0.80	66	LS3	P3	CH

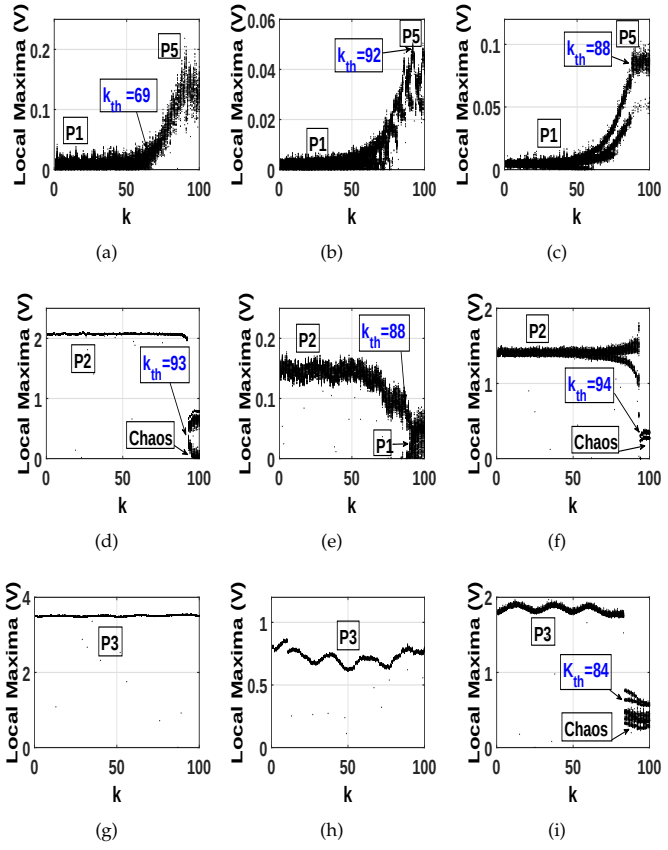

Figure 4 Bifurcation diagrams of the three SLs, under P5 periodic injected signal from the ML. The figures corresponds to the information shown in Table 2

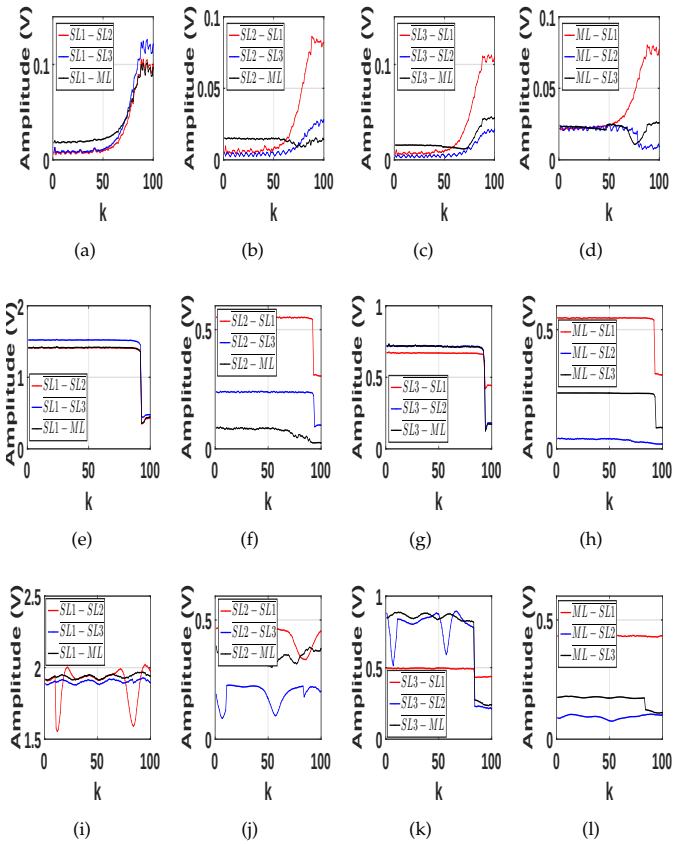

Figure 5 Average values of difference between: a) SL 2 (red color), SL 3 (blue color) and ML (black color) from SL 1, b) SL 1 (red color), SL 3 (blue color) and ML (black color) from SL 2, c) SL 1 (red color), SL 2 (blue color) and ML (black color) from SL 3, and d) SL 1 (red color), SL 2 (blue color) and SL 3 (black color) from ML laser.

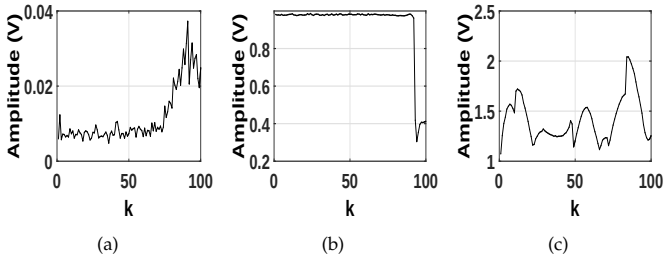

Figure 6 Average values of sum of the three SLs time series for each coupling strength value (k).

revised. The Figure 7 shows the bifurcation diagrams of local maxima of time series for the three driving lasers (SL). Each of the SLs has been modulated by the driver laser (ML) with a previously fixed signal in P4 behavior, this can be obtained by changing the initial condition by turning on and off the function generator. Having fixed the ML in a P4 behavior, it has been applied a coupling strength k variation between the ML and each of the SLs (for SL1, SL2, and SL3). From obtained results, in Table 2 its possible to observe that the coupling value k, and the modulation amplitude are not the same, it is because the differences between the SL behaviors that can be apreciated from Fig. 3. As result of the coupling strength between the ML and the SLs, also it is possible to see that the final behavior is not a tracking attractor between ML and SLs. For the case that the SLs are initially in P1, Fig 7(a–c), the final obtained behavior corresponds to P4, here it worths to mention that P4 is not a possible behavior in those lasers, but the SLs reach the tracking attractor. For the coupling with SLs with a behavior

different from P1, i.e. P2, see Figs. 7(d–f), and P3, see Figs. 7(g–i), the resulting behavior does not completely follow the P4 attractor, and aditionally, in some cases, it is chaotic.

Table 3 Behavior of the SL for threshold k for ML P4 oscillation.

Figure	threshold k	Amplitude (V)	Modulation frequency (kHz)	LS number	Initial behavior	Final behavior
7 (a)	74	0.80	110	LS1	P1	P4
7 (b)	84	1.40	110	LS2	P1	P4
7 (c)	61	1.00	110	LS3	P1	P4
7 (d)	96	0.80	66	LS1	P2	CH/P3
7 (e)	92 and 97	1.40	65	LS2	P2	CH/P4
7 (f)	95	1.00	66	LS3	P2	CH
7 (g)	73 and 85	0.80	66	LS1	P3	CH/P3
7 (h)	86	0.80	66	LS2	P3	CH
7 (i)	76	0.80	66	LS3	P3	CH

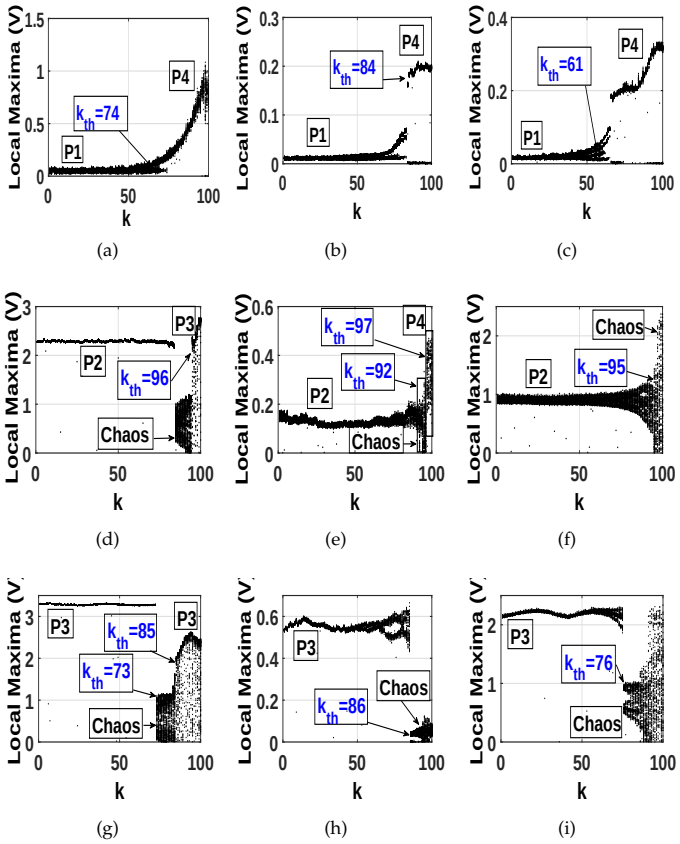

Figure 7 Bifurcation diagrams of the three SLs, under P5 periodic injected signal from the ML. The figures corresponds to the information shown in Table 3

A comparision between the SLs is realized to know the obtained behavior after the ML perturbation. In order to see if the arrangement of three SLs reach the tracking attractor of the ML, the average values of their intensities differences has been done. When the value is close to zero, it implies the tracking attractor between ML and SLs, see Fig. 8.

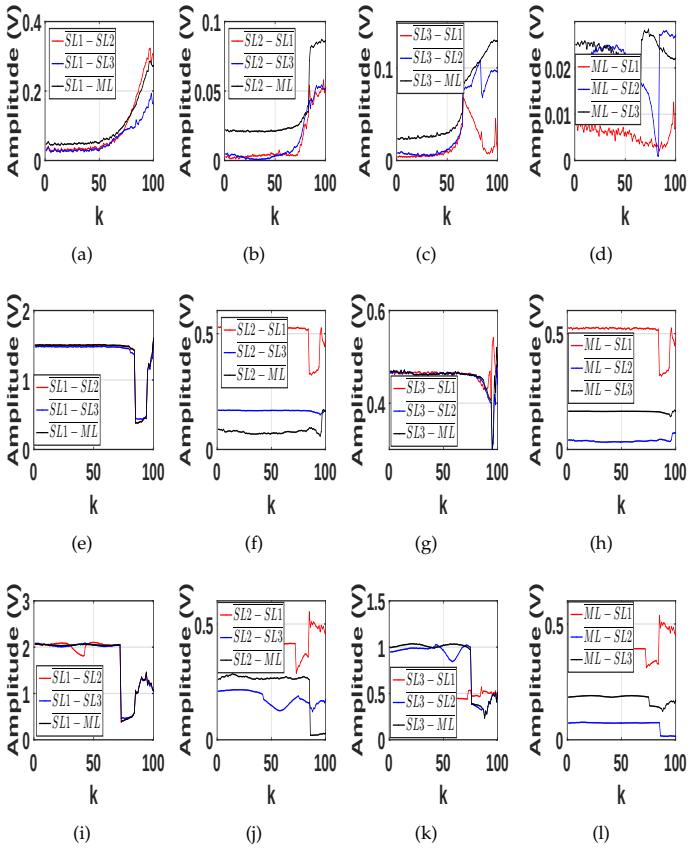

Figure 8 Average values of difference between: a) SL 2 (red color), SL 3 (blue color) and ML (black color) from SL 1, b) SL 1 (red color), SL 3 (blue color) and ML (black color) from SL 2, c) SL 1 (red color), SL 2 (blue color) and ML (black color) from SL 3, and d) SL 1 (red color), SL 2 (blue color) and SL 3 (black color) from ML laser.

In order to compare the obtained results from the optical injection of the ML to the SLs, the sums of the resulting behaviors of the SLs are achieved. In Fig. 9(a-d), it is possible to see from the obtained results, that in the case of SLs with initial behavior of P1, the similitude does not have a big change, while with the other initial states the results are too different between the SLs and the ML.

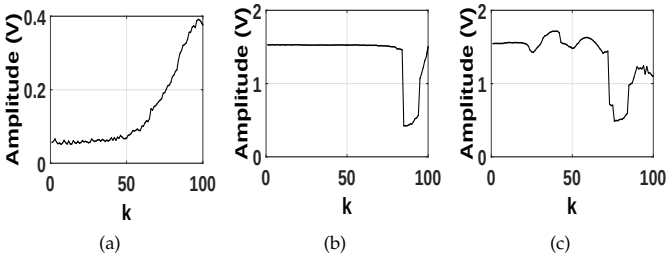

Figure 9 Average values of sum of the three SLs time series for each coupling strength value (k).

CONCLUSIONS

By considering that the SLs have different global behavior, as can be confirmed from Figure 3, the analysis of their answer to the same optical injection was made. The construction of the bifurcation diagram and basin of attraction of the coexistent states of EDFL, allowed us to know the multistable behavior in the driver laser output signal. The output signal from the ML was implemented as additional modulation to the pump power of the three multistable SLs array and in turn. The results obtained when the ML injects a P5, and P4 dynamical behavior shows an attractor tracker response, in this sense when SLs have P1 dynamics a phase synchronization to a single state is favored. This synchronization phenomenon has been reported and studied from other authors by different coupling techniques in other type of lasers, but in one-to-one coupling. In the case of synchronized lasers, a result through the suitable choice of the coupling strength value and the sum of the output signals of the three slave lasers allowed us to obtain maximal power. This optimal power crucially depends on the $k_{threshole}$ value.

Results obtained when the SLs have an initial behavior of P2, shown chaos and P1 monostable behavior when the ML operates in P5. In the case of P1 response, is a possible effect related with one of the three actual behavior of the SL but the answer of chaos reserves another analysis related with the interaction of different periodic states. The obtained results of the injected SLs when the ML is oscillating in P4, shown a richer dynamics in the case when bistable behavior of CH/P3, and CH/P4 is obtained. The activity of P4 is more related to harmonic behavior from the I.C. of the SL, while the P3 is one of the possible dynamics of the SLs.

The presented results are just an analysis of the possible answer of the SLs, that are implemented with the same erbium doped fiber, and the differences on the dynamical behavior are because this systems are real and the small differences in the erbium concentration can produce changes in the final result, as the chaos theory affirms. In this sense, more analysis and research could be implemented. In the case of SLs synchronized with the ML in P5 behavior, we consider that one possible application is in the repeaters of communication systems.

Acknowledgments

J.O.E. thanks Consejo Nacional de Ciencia y Tecnologia (CONACyT) for support provided to develop the studies of Doctorate in Science and Technology at CULagos in UdeG. R.J.-R. thanks CONACYT for financial support, project No. 320597. To AMVP, and VPS for their support with the final edition of the paper.

Availability of data and material

Not applicable.

Conflicts of interest

The authors declare that there is no conflict of interest regarding the publication of this paper.

LITERATURE CITED

Barba-Franco, J., L. Romo-Muñoz, R. Jaimes-Reátegui, J. García-López, G. Huerta-Cuellar, *et al.*, 2023 Electronic equivalent of a pump-modulated erbium-doped fiber laser. Integration **89**: 106–113.

Bouzid, B., 2011 New erbium doped fiber laser amplifier. In *2011 Saudi International Electronics, Communications and Photonics Conference (SIECPC)*, pp. 1–3, IEEE.

Cai, X., P. Gu, and Z. Zhang, 2022 Real-time observation of mode locking and q-switching in erbium-doped fiber laser using plasmonic titanium nitride nanoparticles. Journal of Russian Laser Research **43**: 169–175.

Castillo-Guzmán, A., G. Anzueto-Sánchez, R. Selvas-Aguilar, J. Estudillo-Ayala, R. Rojas-Laguna, *et al.*, 2008 Erbium-doped tunable fiber laser. In *Laser Beam Shaping IX*, volume 7062, pp. 214–217, SPIE.

Digonnet, M., 2001 *Rare-Earth-Doped Fiber Lasers and Amplifiers, Revised and Expanded*. CRC, second edition.

Doumbia, Y., T. Malica, D. Wolfersberger, K. Panajotov, and M. Sciamanna, 2020 Nonlinear dynamics of a laser diode with an injection of an optical frequency comb. Opt. Express **28**: 30379–30390.

Doumbia, Y., D. Wolfersberger, K. Panajotov, and M. Sciamanna, 2022 Two polarization comb dynamics in vcsels subject to optical injection. In *Photonics*, volume 9, p. 115, MDPI.

Droste, S., G. Ycas, B. R. Washburn, I. Coddington, and N. R. Newbury, 2016 Optical frequency comb generation based on erbium fiber lasers. Nanophotonics **5**: 196–213.

Duarte, F., 2009 *Tunable Laser Applications*. CRC, second edition.

Esqueda-de-la Torre, J., J. García-López, G. Huerta-Cuellar, and R. Jaimes-Reategui, 2022 Synchronization of two fiber lasers with optical logarithmic coupler: Experimental implementation. In *Complex Systems and Their Applications*, pp. 3–21, Springer.

Huang, Y., P. Zhou, Y. Zeng, R. Zhang, and N. Li, 2022 Evolution of extreme events in a semiconductor laser subject to chaotic optical injection. Physical Review A **105**: 043521.

Huerta-Cuellar, G., A. Pisarchik, A. Kir'yanov, Y. O. Barmenkov, and J. del Valle Hernández, 2009 Prebifurcation noise amplification in a fiber laser. Physical Review E **79**: 036204.

Huerta-Cuellar, G., A. N. Pisarchik, and Y. O. Barmenkov, 2008 Experimental characterization of hopping dynamics in a multistable fiber laser. Physical Review E **78**: 035202.

Jafry, A., N. Kasim, M. Rusdi, A. Rosol, R. Yusoff, *et al.*, 2020 Max phase based saturable absorber for mode-locked erbium-doped fiber laser. Optics & Laser Technology **127**: 106186.

Keren, S. and M. Horowitz, 2001 Interrogation of fiber gratings by use of low-coherence spectral interferometry of noiselike pulses. Optics Letters **26**: 328–330.

Kir'yanov, A. V., Y. O. Barmenkov, G. E. Sandoval-Romero, and L. Escalante-Zarate, 2013 er^{3+} concentration effects in commercial erbium-doped silica fibers fabricated through the mcvd and dnd technologies. IEEE Journal of Quantum Electronics **49**: 511–521.

Kraus, M., M. A. Ahmed, A. Michalowski, A. Voss, R. Weber, *et al.*, 2010 Microdrilling in steel using ultrashort pulsed laser beams with radial and azimuthal polarization. Optics express **18**: 22305–22313.

Lim, H., Y. Jiang, Y. Wang, Y.-C. Huang, Z. Chen, *et al.*, 2005 Ultrahigh-resolution optical coherence tomography with a fiber laser source at 1 μm. Optics letters **30**: 1171–1173.

Liu, J., X. Li, J. Feng, C. Zheng, Y. Wang, *et al.*, 2020 Zns nanospheres for optical modulator in an erbium-doped fiber laser. Annalen der Physik **532**: 1900454.

Luo, L. and P. Chu, 1998 Optical secure communications with chaotic erbium-doped fiber lasers. J. Opt. Soc. Amer. B **15**: 2524–2530.

Magallón, D. A., R. Jaimes-Reátegui, J. H. García-López, G. Huerta-Cuellar, D. López-Mancilla, *et al.*, 2022 Control of multistability in an erbium-doped fiber laser by an artificial neural network: A numerical approach. Mathematics **10**: 3140.

Morin, F., F. Druon, M. Hanna, and P. Georges, 2009 Microjoule

femtosecond fiber laser at 1.6 μm for corneal surgery applications. Optics letters **34**: 1991–1993.

Philippov, V., C. Codemard, Y. Jeong, C. Alegria, J. K. Sahu, *et al.*, 2004 High-energy in-fiber pulse amplification for coherent lidar applications. Optics letters **29**: 2590–2592.

Pisarchik, A. and R. Jaimes-Reategui, 2009 Control of basins of attraction in a multistable fiber laser. Physics Letters A **374**: 228–234.

Pisarchik, A., R. Jaimes-Reátegui, R. Sevilla-Escoboza, and G. Huerta-Cuellar, 2012 Multistate intermittency and extreme pulses in a fiber laser. Physical Review E **86**: 056219.

Pisarchik, A., R. Sevilla-Escoboza, R. Jaimes-Reátegui, G. Huerta-Cuellar, J. García-Lopez, *et al.*, 2013 Experimental implementation of a biometric laser synaptic sensor. Sensors pp. 17322–17331.

Pisarchik, A. N. and A. E. Hramov, 2022 Multistability in lasers. In *Multistability in Physical and Living Systems*, pp. 167–198, Springer.

Pisarchik, A. N., R. Jaimes-Reátegui, R. Sevilla-Escoboza, G. Huerta-Cuellar, and M. Taki, 2011 Rogue waves in a multistable system. Physical Review Letters **107**: 274101.

Pisarchik, A. N., A. V. Kir'yanov, Y. O. Barmenkov, and R. Jaimes-Reátegui, 2005 Dynamics of an erbium-doped fiber laser with pump modulation: theory and experiment. JOSA B **22**: 2107–2114.

R. Mary, D. C. and A. Kar, 2014 Eapplications of fiber lasers for the development of compact photonic devices. IEEE J. Sel. Top. Quantum Electron **20**: 0902513.

Reategui, R., A. Kir'yanov, A. Pisarchik, Y. O. Barmenkov, and N. Il'ichev, 2004 Experimental study and modeling of coexisting attractors and bifurcations in an erbium-doped fiber laser with diode-pump modulation. Laser Phys **14**: 1277–1281.

Sevilla-Escoboza, R., G. Huerta-Cuéllar, R. Jaimes-Reátegui, J. García-López, C. Medel-Ruiz, *et al.*, 2017 Error-feedback control of multistability. Journal of the Franklin Institute **354**: 7346–7358.

Soboń, G., 2022 Noise-like pulses in mode-locked fiber lasers. In *Dissipative Optical Solitons*, pp. 319–337, Springer.

Tseng, C.-H., J.-H. Yang, and S.-K. Hwang, 2022 Numerical study of noise-induced transitions in nonlinear dynamics of optically injected semiconductor lasers. Nonlinear Theory and Its Applications, IEICE **13**: 60–71.

Wu, Q., Y. Okabe, and J. Sun, 2014 Investigation of dynamic properties of erbium fiber laser for ultrasonic sensing. Optics express **22**: 8405–8419.

Xu, L., L. Zhang, Z. Zhang, Z. Gao, J. Tian, *et al.*, 2022 Conventional soliton dynamics of mode-locked erbium-doped fiber lasers. In *Second Optics Frontier Conference (OFS 2022)*, volume 12307, pp. 35–39, SPIE.

Zhao, L., D. Li, L. Li, X. Wang, Y. Geng, *et al.*, 2017 Route to larger pulse energy in ultrafast fiber lasers. IEEE Journal of Selected Topics in Quantum Electronics **24**: 1–9.

How to cite this article: Esqueda-de-la-Torre, J. O., Jaimes-Reátegui, R., García-López, J. H., Pisarchik, A. N., and Huerta-Cuellar, G. Effects of Optical Laser Injection in Multistable Erbium Fiber Lasers. *Chaos Theory and Applications*, 4(4), 226-233, 2022.